# Distinct molecular mechanism for initiating TRAF6 signalling

**Hong Ye*†, Joseph R. Arron†‡§, Betty Lamothe||¶, Maurizio Cirilli*#, Takashi Kobayashi§, Nirupama K. Shevde☆, Deena Segal*, Oki K. Dzivenu*, Masha Vologodskaia**, Mijung Yim§, Khoi Du||, Sujay Singh††, J. Wesley Pike☆, Bryant G. Darnay||, Yongwon Choi§ & Hao Wu***

** Department of Biochemistry, Weill Medical College of Cornell University, New York, New York 10021, USA*
*‡ Tri-Institutional MD-PhD Program, and ** Laboratory of Immunology, The Rockefeller University, New York, New York 10021, USA*
*§ Abramson Family Cancer Research Institute, Department of Pathology and Laboratory Medicine, University of Pennsylvania School of Medicine, Philadelphia, Pennsylvania 19104, USA*
*|| Department of Bioimmunotherapy, The University of Texas MD Anderson Cancer Center, Box 143, 1515 Holcombe Boulevard, Houston, Texas 77030, USA*
*# Istituto di Strutturistica Chimica 'Giordano Giacomello', CNR, CP 10, Monterotondo Stazione, Italy*
*☆ Department of Biochemistry, University of Wisconsin, Madison, Wisconsin 53706, USA*
*†† Imgenex Corporation, 11185 Flintkote Ave, Suite E, San Diego, California 92121, USA*
*† These authors contributed equally to this work*

**Tumour-necrosis factor (TNF) receptor-associated factor 6 (TRAF6) is the only TRAF family member that participates in signal transduction of both the TNF receptor (TNFR) superfamily and the interleukin-1 receptor (IL-1R)/Toll-like receptor (TLR) superfamily[1–5]; it is important for adaptive immunity, innate immunity and bone homeostasis. Here we report crystal structures of TRAF6, alone and in complex with TRAF6-binding peptides from CD40 and TRANCE-R (also known as RANK), members of the TNFR superfamily, to gain insight into the mechanism by which TRAF6 mediates several signalling cascades. A 40° difference in the directions of the bound peptides in TRAF6 and TRAF2 shows that there are marked structural differences between receptor recognition by TRAF6 and other TRAFs. The structural determinant of the petide–TRAF6 interaction reveals a Pro-X-Glu-X-X-(aromatic/acidic residue) TRAF6-binding motif, which is present not only in CD40 and TRANCE-R but also in the three IRAK adapter kinases for IL-1R/TLR signalling. Cell-permeable peptides with the TRAF6-binding motif inhibit TRAF6 signalling, which indicates their potential as therapeutic modulators. Our studies identify a universal mechanism by which TRAF6 regulates several signalling cascades in adaptive immunity, innate immunity and bone homeostasis.**

The unique biological function of TRAF6 is largely determined by its TRAF-C domain, which does not interact with peptide motifs that are recognized by TRAF1, -2, -3 or -5 (refs 6–8). To elucidate the molecular basis of TRAF6 specificity, we determined the crystal structures (Table 1 and Fig. 1a) of the TRAF-C domain (residues 346–504) alone and in complex with a peptide from human CD40 (residues 230–238, KQEPQEIDF)[9] or TRANCE-R (residues 342–349, QMPTEDEY)[10]. The CD40 peptide contains a mutation (Asn237Asp) that enhances affinity to TRAF6 (ref. 11). Using isothermal titration calorimetry (ITC), we determined the dissociation constant ($K_d$) between TRAF6 and the nine-residue CD40 peptide to be 84 μM, which is essentially the same as the $K_d$ between TRAF6 and the whole intracellular segment of CD40 (Supplementary Information). A low affinity between TRAF6 and monomeric receptors is expected, because TRAF recruitment is dependent on affinity enhancement by receptor and adapter protein oligomerization[5,12].

Unexpectedly, there are marked differences in peptide binding to TRAF6 and to other TRAFs. First, the chain direction of bound TRAF6-binding peptides shows a 40° difference to that of TRAF2-binding peptides (Fig. 1b–d). As a result, side chains of TRAF6-binding peptides interact with surface pockets on TRAF6 that are completely different from those on TRAF2. Second, the TRAF6-binding peptides assume extended β-conformations, rather than the poly-proline II (PPII) helix conformation for the core region of TRAF2-binding peptides (Fig. 1b). The peptides also make more extensive main-chain hydrogen bonds with the TRAF-C domain β7 strand (residues 234–238 of CD40 and 344–349 of TRANCE-R with residues Pro 468 to Gly 472 of TRAF6), which carries the Pro 468 insertion in its β-bulge (Fig. 1e). Finally, the peptides do not interact with the β3–β4 loop in the TRAF6 complexes, owing to a movement of 12 Å in the position of this loop (Fig. 1b).

Similar to the nomenclature used for TRAF2-binding peptides, which bear the consensus (Pro/Ser/Thr/Ala)-X-(Gln/Glu)-Glu (corresponding to $P_{-2}$ to $P_1$; Fig. 1d), we denote residues Glu 235 of CD40 and Glu 346 of TRANCE-R as the $P_0$ position of TRAF6-binding peptides because they occupy a similar, but not identical, location to the $P_0$ residue (Gln/Glu) in the TRAF2-binding motif (corresponding Cα distance 2.3 Å). The $P_0$ position is near the point of intersection between the two classes of peptide. For the peptide residues in contact with TRAF6 ($P_{-4}$ to $P_3$), analyses of surface area burial and specific side-chain interactions suggest that the $P_{-2}$, $P_0$ and $P_3$ residues contribute most to the structural interaction (Fig. 1g).

The different surface pocket for the $P_{-2}$ residue seems to be an important factor in determining the different mode of peptide binding by TRAF6 relative to TRAF2. Ser 467 and Cys 469, which form the $P_{-2}$ pocket in TRAF2, are replaced in TRAF6 by Phe 471 and Tyr 473, which form an alternative pocket for the $P_{-2}$ proline residue that is located about 3 Å from that in TRAF2 (Fig. 1c–e). The carboxylate of the $P_0$ glutamic acid residue is recognized by hydrogen bonding with main-chain amide nitrogen atoms of Leu 457 and Ala 458, and the aliphatic portion of the side chain shows a close fit with the TRAF6 surface (Fig. 1c, e). This mode of interaction is in contrast to the recognition of the $P_0$ glutamic acid/glutamine by the hydroxyls of three serine residues (453–455) in TRAF2. In addition, the carboxylate of the $P_0$ residue may form a favourable charge–charge interaction with the side chain of Lys 469, although the interaction is not within hydrogen-bonding distance. The $P_3$ residue, Phe 238 of CD40 or Tyr 349 of TRANCE-R, is adjacent to several aromatic and basic residues of TRAF6 (Fig. 1e). An amino–aromatic interaction is observed between Tyr 349 of TRANCE-R and Arg 392 of TRAF6. Structurally, a similar interaction should be possible for either Phe 238 of CD40 or an acidic residue, which is present in mouse CD40 (Fig. 1g). The observed difference in the side-chain conformation of the $P_3$ residue in CD40 is probably caused by crystal packing (Fig. 1f).

Structure-based sequence alignment of TRAF6-binding sites in human and mouse CD40 and TRANCE-R led to the definition of a TRAF6-binding motif for $P_{-2}$ to $P_3$ of Pro-X-Glu-X-X-(Ar/Ac), where Ar is an aromatic and Ac an acidic residue (Fig. 1g). An *in vitro* binding assay between glutathione *S*-transferase (GST)-fused full-length cytoplasmic domain of CD40 (GST–CD40ct) and TRAF6 (residues 333–508) confirmed the structural prediction that the $P_{-2}$, $P_0$ and $P_3$ residues are the most crucial for TRAF6 interaction (Fig. 1g). Similarly, in a cellular assay of the ability of CD40 to activate the NF-κB transcription factor[11], mutations of the same three residues significantly decreased NF-κB reporter activity as compared with wild-type CD40 (Fig. 2a). The $P_1$ and $P_2$ positions may have a preference for acidic residues owing to their complementarity to the basic TRAF6 surface (Fig. 1c), which is formed in particular by the side chains of Arg 392 and Lys 469 at this region.

¶ Present address: Department of Pharmacology, Yale University, New Haven, Connecticut 06520, USA.

**Table 1 Crystallographic statistics**

| Crystal | Native | hCD40 complex | hTRANCE-R complex |
|---|---|---|---|
| TRAF6 | Residues 346–504 | Residues 346–504 | Residues 346–504 |
| Peptide | None | 230-KQEPQEIDF | 342-QMPTEDEY |
| Space group | $P2_1$ | $P2_12_12_1$ | $P2_12_12_1$ |
| Cell dimensions | $a = 32.2$ Å, $b = 55.6$ Å, $c = 47.7$ Å, $\beta = 101.0°$ | $a = 39.9$ Å, $b = 43.8$ Å, $c = 101.4$ Å | $a = 38.0$ Å, $b = 45.0$ Å, $c = 106.5$ Å |
| Diffraction data | | | |
| Resolution | 40–2.4 Å | 40–1.8 Å | 40–2.0 Å |
| $R_{sym}$ (last shell) | 9.2% (24.1%) | 5.6% (22.1%) | 5.5% (13.9%) |
| Completeness (last shell) | 92.8% (90.4%) | 99.1% (93.0%) | 96.0% (86.9%) |
| Refinement | | | |
| Resolution | 20–2.4 Å | 20–1.8 Å | 20–2.0 Å |
| Sigma cut-off | 2.0 | 2.0 | 2.0 |
| Number of protein residues | 155 | 164 | 161 |
| Number of protein atoms | 1,269 | 1,340 | 1,331 |
| Number of solvent atoms | 45 | 122 | 80 |
| Number of reflections used | 5,538 | 14,644 | 12,396 |
| $R$ ($R_{free}$) | 20.4% (27.4%) | 20.3% (25.8%) | 21.3% (24.2%) |
| r.m.s. deviation bond length | 0.007 Å | 0.014 Å | 0.005 Å |
| r.m.s. deviation bond angle | 1.4° | 1.8° | 1.3° |

ITC measurements showed that peptides with acidic residues at these positions possess higher affinity to TRAF6 (Supplementary Information).

However, mutations of the $P_{-2}$, $P_0$ and $P_3$ residues of the TRANCE-R sequence in the full-length receptor failed to reduce TRANCE-R-induced NF-κB activation (ref. 13 and Supplementary Information). Examination of the TRANCE-R sequence suggested that there are three potential TRAF6-binding sites (Fig. 1g, h). To evaluate the functional roles of these sites, we generated single, double and triple mutations at each of the $P_0$ positions to disrupt one, two or three of the TRAF6-binding sites (Fig. 2b). Neither single nor double mutations resulted in a significant reduction of NF-κB activation; however, the triple mutation reduced NF-κB reporter activity to less than 20% of that of wild-type TRANCE-R, which suggests that the three sites are redundantly involved in TRAF6 interaction and signal transduction. The remaining NF-κB activity induced by the triple TRANCE-R mutant can be attributed to the presence of TRAF2-binding sites in full-length TRANCE-R. It

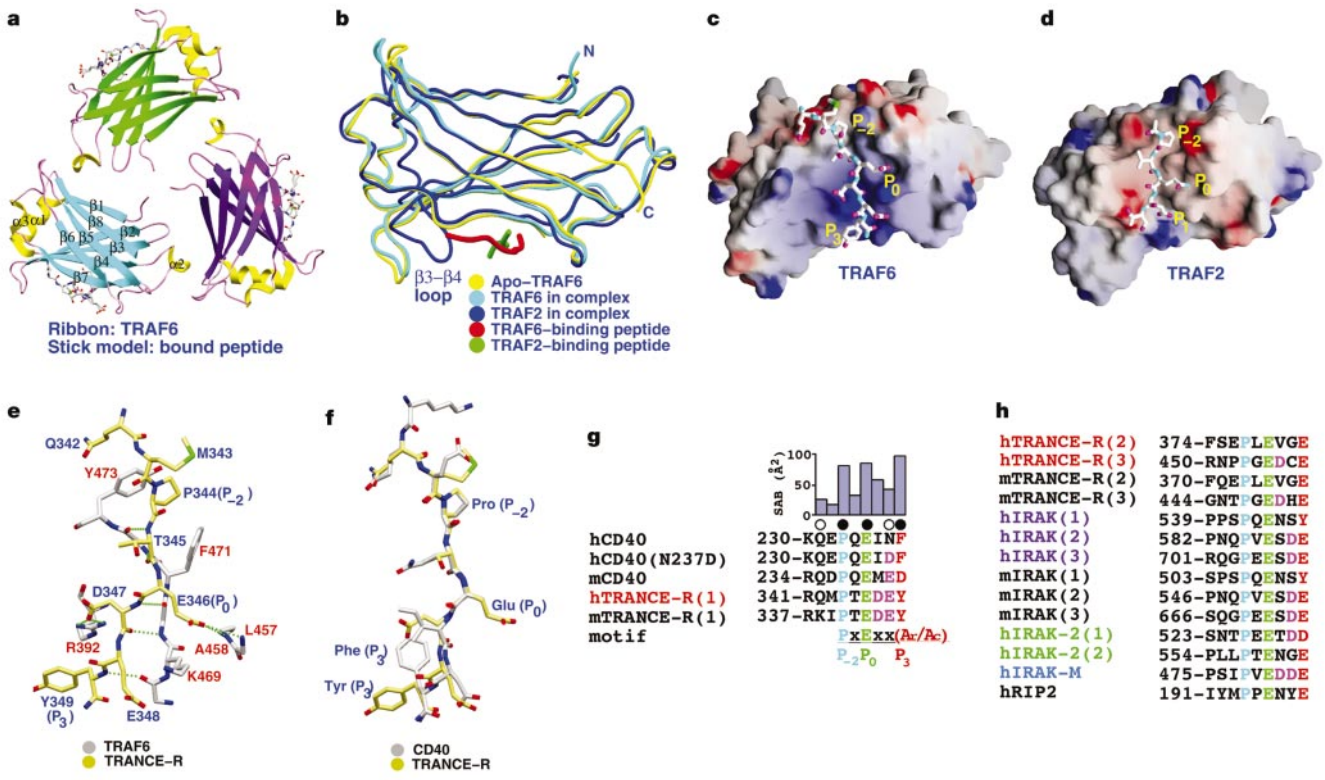


**Figure 1** TRAF6 structures. **a**, Ribbon diagram of the TRAF domain of TRAF6 in complex with TRANCE-R, shown as a trimeric model by applying the putative three-fold symmetry observed in TRAF2 structures[6]. **b**, Worm Cα traces of superimposed TRAF6 and TRAF2 structures. **c**, Surface representation of TRAF6, coloured on the basis of electrostatic potential ($-10k_bT/e$ to $+10k_bT/e$, where $k_b$, $T$ and $e$ are the Boltzmann constant, temperature and the electron charge, respectively), and the bound TRANCE-R peptide. **d**, Surface representation of TRAF2, shown with the bound core CD40 peptide. **e**, Interaction between TRAF6 and the TRANCE-R peptide. Main-chain hydrogen bonds between the TRANCE-R peptide and the β7 strand of TRAF6 are shown as dotted lines. Side chains of some of the β7 residues are omitted for clarity. **f**, Superposition of the TRANCE-R and the CD40 peptide. **g**, The Pro-X-Glu-X-X-(Ar/Ac) TRAF6-binding motif. The surface area buried (SAB) on TRAF6 interaction for the eight contacting residues ($P_{-4}$ to $P_3$) is shown. CD40 residues that were mutated to assess their effect on *in vitro* interaction with TRAF6 are indicated on top by a circle (open, does not abolish interaction; filled, abolishes interaction). **h**, Presence of one or many Pro-X-Glu-X-X-(Ar/Ac) motifs in TRANCE-R, IRAK, IRAK-2, IRAK-M and RIP2.

is possible that the presence of several TRAF6-binding sites in TRANCE-R increases the probability of TRAF6 recruitment and explains the dominant role of TRAF6 in TRANCE-R signalling[2,3].

The best-characterized TRAF6 signalling pathway for the IL-1R/TLR superfamily involves IRAK, an adapter kinase upstream of TRAF6 (refs 1, 14, 15 and Fig. 1h). On receptor stimulation, IRAK becomes oligomerized and interacts with TRAF6 (ref. 12). Full-length IRAK contains three potential TRAF6-binding sites (Fig. 1h), which suggests that it may directly initiate TRAF6 signalling through the same structural mechanism. To test the functional importance of these sites, we generated a series of single, double and triple mutations of the respective $P_0$ residues (Fig. 2c). On transfection, wild-type IRAK strongly promoted NF-κB reporter activity, whereas single, double and triple $P_0$ mutations attenuated NF-κB activity relative to the wild type. The degree of attenuation increased with the number of $P_0$ mutations, with the triple mutation showing NF-κB activation that was close to the background activation. All of the IRAK mutants showed similar amounts of expression (Supplementary Information). These observations suggest that the three TRAF6-binding sites in IRAK contribute collectively to TRAF6 activation.

The identification of the Pro-X-Glu-X-X-(Ar/Ac) motif prompted us to inspect sequences of other proteins that may directly interact with TRAF6 (Fig. 1h). We found that the IRAK homologues IRAK-M[12] and IRAK-2 (ref. 16) contain, respectively, one and two potential TRAF6-binding sites. This is in keeping with the implicated role of IRAK-2 and IRAK-M in IL-1 signalling[12,16] and the role of IRAK-2 in TLR4 signalling[17,18]. In addition, we found that the kinase RIP2, which can activate NF-κB and induce cell death[19], also contains a putative TRAF6-binding site.

We showed further that the direct interaction between TRAF6 and the Pro-X-Glu-X-X-(Ar/Ac) motifs in IRAK and IRAK homologues is responsible for initiating TRAF6 signal transduction under endogenous conditions using dominant-negative TRAF6 (T6.DN) with a mutation at Arg 392, Phe 471 or Tyr 473. Whereas wild-type T6.DN could compete with and downregulate endogenous IL-1-induced TRAF6 signalling, the mutant T6.DN proteins, which failed to interact with the Pro-X-Glu-X-X-(Ar/Ac) motif *in vitro* (Supplementary Information), showed significantly reduced inhibition of NF-κB activation (Fig. 2d). All T6.DN mutants were expressed in similar quantities (Supplementary Information).

We tested whether peptides derived from the TRAF6-interacting motif could inhibit TRAF6-mediated signal transduction. We generated cell-permeable decoy peptides, L-T6DP-1 and L-T6DP-

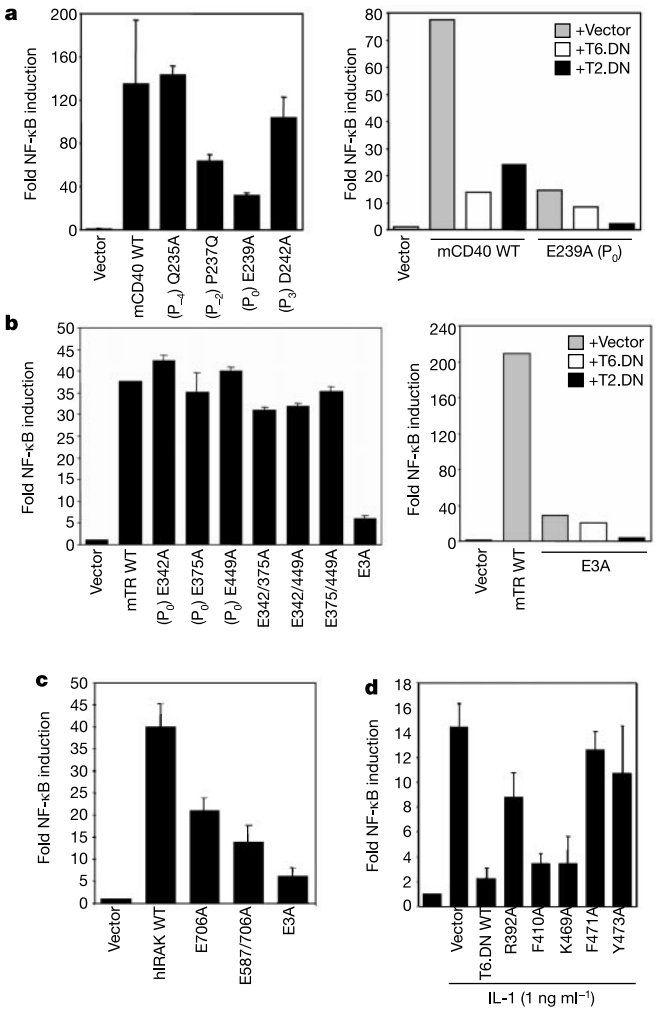


**Figure 2** Functional analyses for the interaction of TRAF6 with CD40, TRANCE-R and IRAK. **a**, NF-κB induction by mouse CD40. **b**, NF-κB induction by mouse TRANCE-R (mTR). **c**, NF-κB induction by human IRAK. **d**, Inhibition of endogenous IL-1 signalling by mouse T6.DN (residues are numbered on the basis of human TRAF6).

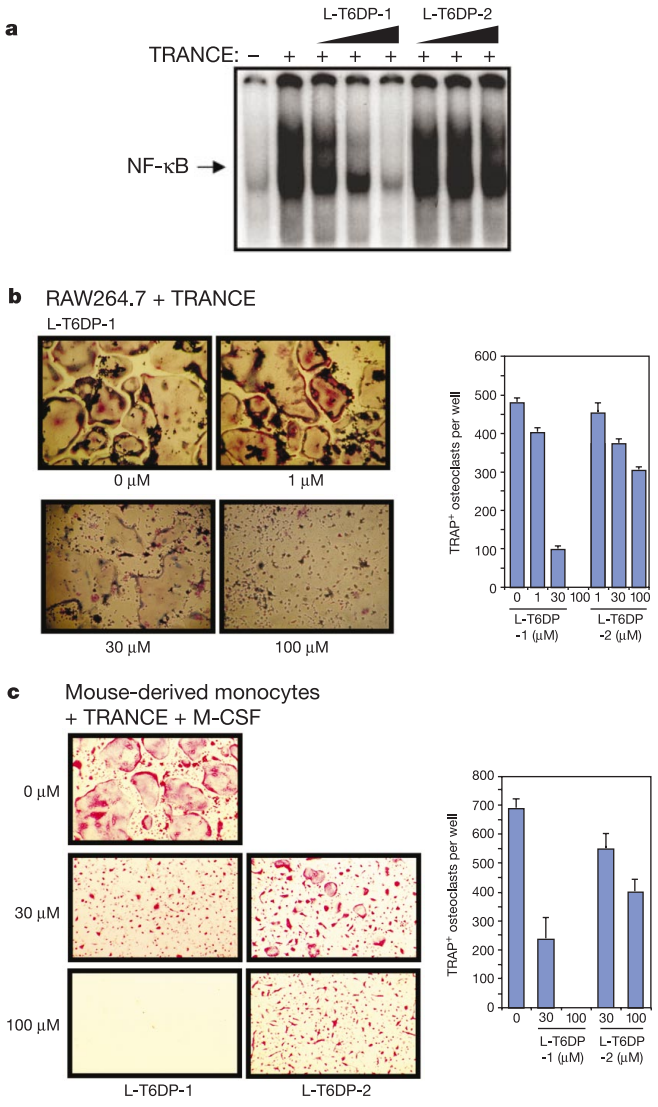


**Figure 3** Inhibitory effects of TRAF6 decoy peptides (L-T6DP-1 and L-T6DP-2) in TRANCE-mediated signal transduction and osteoclast differentiation. **a**, Inhibition of TRANCE-mediated NF-κB activation by TRAF6 decoy peptides, as shown by EMSA. **b**, **c**, Inhibition of TRANCE-mediated osteoclast differentiation in RAW264.7 cells (**b**) and primary monocytes (**c**) by TRAF6 decoy peptides. Cells were stained for TRAP.

2, by fusing a hydrophobic sequence of the Kaposi fibroblast growth factor signal peptide[20] with sequences containing TRANCE-R(1) and TRANCE-R(2), respectively (Fig. 1g, h). TRANCE-R(2) does not contain acidic residues at either the $P_1$ or $P_2$ position, which may explain why it shows a much weaker affinity for TRAF6 than that of TRANCE-R(1), as measured by ITC ($K_d$, 770 μM and 78 μM, respectively).

We used RAW264.7 cells, which express endogenous TRANCE-R, to test the effects of the decoy peptides, because it is desirable to block TRANCE-R-mediated osteolytic activity[21] in many human diseases such as osteoporosis and cancer-induced bone lesions. Pre-treatment with L-T6DP-1 inhibited endogenous TRANCE-R-mediated NF-κB activation on TRANCE stimulation in a dose-dependent manner (Fig. 3a). The effective concentration of L-T6DP-1 is consistent with the affinity between TRANCE-R(1) and TRAF6. The L-T6DP-2 peptide did not produce detectable inhibition of NF-κB activation, which is consistent with the much weaker affinity of TRANCE-R(2) for TRAF6 and indicates the specific effects of these peptides.

We further tested whether TRANCE-induced osteoclast differentiation can be blocked by TRAF6-binding decoy peptides in a model cell line and in primary cells. After stimulation with TRANCE and TRANCE plus macrophage colony-stimulating factor (M-CSF), respectively, RAW264.7 cells and primary mouse-derived monocytes differentiated into multinucleated, tartrate-resistant acid phosphatase (TRAP)-positive osteoclasts. Co-treatment of RAW264.7 cells and primary monocytes with L-T6DP-1 or L-T6DP-2 caused a dose-dependent decrease of TRAP-positive osteoclasts (Fig. 3b, c) without affecting cell viability (Supplementary Information). These results show that peptides containing the TRAF6-binding motif can act as decoys to inhibit TRAF6 signalling and its associated biological functions.

In summary, our structural and functional study identifies a universal structural mechanism by which TRAF6 participates in adaptive immunity, innate immunity and bone homeostasis. This molecular understanding provides not only insights into the signalling mechanism, but also tools to modulate TRAF6-mediated biological processes. □

## Methods

### Protein expression, purification and crystallization

A combination of genetic, biochemical and crystallographic methods was used to identify a construct of TRAF6 that gives well-diffracting crystals. In brief, we screened many TRAF6 deletions and found that the construct (residues 333–508) containing part of the coiled-coil domain and the whole TRAF-C domain produced soluble protein that existed predominately as trimers in solution. Poorly diffracting crystals could be obtained, but only at very low protein concentrations. Crystal packing revealed by the molecular replacement solution showed that the TRAF6 construct was monomeric in the crystal with presumably a disordered coiled-coil domain. Removal of most of the coiled-coil domain led to a new monomeric TRAF6 construct (residues 346–504), which showed low solubility but produced well-diffracting crystals. Both TRAF6 constructs contain carboxy-terminal histidine tags. They were purified by $Ni^{2+}$-affinity chromatography and gel filtration, and crystallized under 5–25% PEG8000 in 100 mM Tris-HCl (pH 7.5). For co-crystallization, a 10-fold molar excess of TRAF6-binding peptides was included in the crystallization drops.

### Isothermal titration calorimetry

Peptides containing putative TRAF6-binding sequences were synthesized chemically with N-terminal acetylation and C-terminal amidation. The TRAF6 (residues 333–508) and peptide samples were dialysed extensively against 50 mM sodium phosphate at pH 7.5 for at least 2 days at 4 °C to ensure buffer equilibration. Accurate concentrations of the TRAF6 and peptide samples after dialysis were determined by quantitative amino acid analysis. We carried out ITC experiments at 20 °C using a microcalorimetry system (MicroCal). Each peptide (1.0–5.0 mM) was titrated into a TRAF6 sample (0.05–0.1 mM) in roughly 20–45 serial injections. Each titration data set was corrected for heat of dilution, obtained by injecting the peptide into the buffer, and analysed by the ORIGIN software[22].

### Data collection and structure determination

Diffraction data were collected at the X4A beamline of NSLS and the A1 beamline of CHESS and processed with the HKL package[23]. The structures were determined by molecular replacement calculations in the program Replace[24] using a TRAF domain structure of TRAF2 (ref. 8) as a search model after removal of non-conserved side chains. We used the simulated annealing protocol in CNS[25] for structure refinement and the program O[26] for model building. Ribbon and stick models were created using Setor[27] and molecular surface representations were calculated and presented by Grasp[28].

### *In vitro* interaction assay

The interaction of TRAF6 (residues 333–508) with the GST-fused intracellular domain of human CD40 (GST–CD40ct, residues 216–273) was carried out by native PAGE and size-exclusion chromatography. We used the PhastSystem (Pharmacia) and 8–25% gradient polyacrylamide gels for native PAGE, and Superdex 200 HR 10/30 (Pharmacia) for size-exclusion chromatography. GST–CD40ct formed oligomers in solution that could interact with the trimeric TRAF6 construct.

### Transfection and NF-κB reporter assays

Mouse CD40 was cloned by polymerase chain reaction with reverse transcription from whole spleen messenger RNA and inserted into the pFlag–CMV1 vector (Sigma). Construction of Flag-tagged mouse TRANCE-R, and mouse dominant-negative TRAF6 (T6.DN, residues 289–530) and TRAF2 (T2.DN, residues 241–501) have been described[13]. Flag-tagged human IRAK was provided by Z. Cao (Tularik). We transfected 293T HEK cells in six-well plates with wild-type or mutant CD40 (100 ng), TRANCE-R (50 ng), IRAK (100 ng), T6.DN (800 ng) or T2.DN (800 ng) along with an NF-κB–luciferase reporter plasmid (75 ng) and a β-galactosidase plasmid (25 ng) to control for transfection efficiency. Transfection amounts were kept constant by adding empty pFlag–CMV1 vector. Cells were collected 24–30 h after transfection, and reporter activity was assayed as described[13]. Where indicated, cells were treated with 1 ng $ml^{-1}$ recombinant human IL-1 (R & D) 6 h before collection. Relative luciferase activity was normalized for β-galactosidase activity. Representative results of at least three independent transfections were obtained (error bars are shown for duplicates or triplicates at each transfection).

### Decoy peptides

TRAF6-binding sequences from mouse TRANCE-R fused with the hydrophobic sequence from Kaposi fibroblast growth factor signal sequence (L-T6DP-1, *AAVALLPAVLLALLAP*-RKIPTEDEYTDRPSQPST; L-T6DP-2, *AAVALLPAVLLALLAP*-IPPFQEPLEVGEND; leader sequence is shown in italic and the TRAF6-binding motif is underlined) were chemically synthesized and purified by high performance liquid chromatography. We confirmed the molecular mass of each peptide by matrix-assisted laser desorption ionization time-of-flight mass spectrometry.

### Electrophoretic mobility shift assays (EMSA)

We plated RAW264.7 cells into six-well plates, incubated them with L-T6DP-1 or L-T6DP-2 (30 μM, 100 μM and 300 μM) for 5 h, and treated them with 10 nM TRANCE for 15 min. Nuclear extracts were prepared as described[29]. Equivalent amounts of nuclear protein were used in an EMSA reaction with $^{32}$P-labelled NF-κB oligonucleotide from the HIV-LTR as described[29].

### *In vitro* osteoclast differentiation

Primary bone marrow monocytes and RAW264.7 cells were cultured in 48-well dishes at a density of $1 \times 10^5$ cells per well and $2 \times 10^3$ cells per well, respectively. They were treated with 50 ng $ml^{-1}$ TRANCE and 10 ng $ml^{-1}$ M-CSF (for bone marrow monocytes) at the beginning of the culture and during a medium change on day 3 (for bone marrow monocytes). We assessed osteoclast formation by counting the total number of multinucleated (>3 nuclei), TRAP-positive cells per well on day 7 for primary monocytes and on day 5 for RAW264.7 cells[30].

Received 26 February; accepted 14 May 2002; doi:10.1038/nature00888.


1. Cao, Z., Xiong, J., Takeuchi, M., Kurama, T. & Goeddel, D. V. TRAF6 is a signal transducer for interleukin-1. *Nature* **383,** 443–446 (1996).
2. Lomaga, M. A. *et al.* TRAF6 deficiency results in osteopetrosis and defective interleukin-1, CD40, and LPS signalling. *Genes Dev.* **13,** 1015–1024 (1999).
3. Naito, A. *et al.* Severe osteopetrosis, defective interleukin-1 signalling and lymph node organogenesis in TRAF6-deficient mice. *Genes Cells* **4,** 353–362 (1999).
4. Aderem, A. & Ulevitch, R. J. Toll-like receptors in the induction of the innate immune response. *Nature* **406,** 782–787 (2000).
5. Chung, J. Y., Park, Y. C., Ye, H. & Wu, H. All TRAFs are not created equal: common and distinct molecular mechanisms of TRAF-mediated signal transduction. *J. Cell Sci.* **115,** 679–688 (2002).
6. Park, Y. C., Burkitt, V., Villa, A. R., Tong, L. & Wu, H. Structural basis for self-association and receptor recognition of human TRAF2. *Nature* **398,** 533–538 (1999).
7. McWhirter, S. M. *et al.* Crystallographic analysis of CD40 recognition and signalling by human TRAF2. *Proc. Natl Acad. Sci. USA* **96,** 8408–8413 (1999).
8. Ye, H., Park, Y. C., Kreishman, M., Kieff, E. & Wu, H. The structural basis for the recognition of diverse receptor sequences by TRAF2. *Mol. Cell* **4,** 321–330 (1999).
9. Pullen, S. S. *et al.* CD40-tumour necrosis factor receptor-associated factor (TRAF) interactions: regulation of CD40 signalling through multiple TRAF binding sites and TRAF hetero-oligomerization. *Biochemistry* **37,** 11836–11845 (1998).
10. Darnay, B. G., Ni, J., Moore, P. A. & Aggarwal, B. B. Activation of NF-κB by RANK requires tumour necrosis factor receptor-associated factor (TRAF) 6 and NF-κB-inducing kinase. Identification of a novel TRAF6 interaction motif. *J. Biol. Chem.* **274,** 7724–7731 (1999).
11. Pullen, S. S., Dang, T. T., Crute, J. J. & Kehry, M. R. CD40 signalling through tumour necrosis factor receptor-associated factors (TRAFs). Binding site specificity and activation of downstream pathways by distinct TRAFs. *J. Biol. Chem.* **274,** 14246–14254 (1999).
12. Wesche, H. *et al.* IRAK-M is a novel member of the Pelle/interleukin-1 receptor-associated kinase (IRAK) family. *J. Biol. Chem.* **274,** 19403–19410 (1999).
13. Wong, B. R. *et al.* The TRAF family of signal transducers mediates NF-κB activation by the TRANCE receptor. *J. Biol. Chem.* **273,** 28355–28359 (1998).

14. Cao, Z., Henzel, W. J. & Gao, X. IRAK: A kinase associated with the interleukin-1 receptor. *Science* **271,** 1128–1131 (1996).
15. Zhang, F. X. *et al.* Bacterial lipopolysaccharide activates nuclear factor-κB through interleukin-1 signalling mediators in cultured human dermal endothelial cells and mononuclear phagocytes. *J. Biol. Chem.* **274,** 7611–7614 (1999).
16. Muzio, M., Ni, J., Feng, P. & Dixit, V. M. IRAK (Pelle) family member IRAK-2 and MyD88 as proximal mediators of IL-1 signalling. *Science* **278,** 1612–1615 (1997).
17. Fitzgerald, K. A. *et al.* Mal (MyD88-adapter-like) is required for Toll-like receptor-4 signal transduction. *Nature* **413,** 78–83 (2001).
18. Horng, T., Barton, G. M. & Medzhitov, R. TIRAP: an adapter molecule in the Toll signalling pathway. *Nature Immunol.* **2,** 835–841 (2001).
19. McCarthy, J. V., Ni, J. & Dixit, V. M. RIP2 is a novel NF-κB-activating and cell death-inducing kinase. *J. Biol. Chem.* **273,** 16968–16975 (1998).
20. Yan Liu, X. *et al.* Peptide-directed suppression of a pro-inflammatory cytokine response. *J. Biol. Chem.* **275,** 16774–16778 (2000).
21. Arron, J. R. & Choi, Y. Bone versus immune system. *Nature* **408,** 535–536 (2000).
22. Bundel, D. R. & Sigurskjold, B. W. Determination of accurate thermodynamics of binding by titration microcalorimetry. *Methods Enymol.* **247,** 288–305 (1987).
23. Otwinowski, Z. & Minor, W. Processing of X-ray diffraction data collected in oscillation mode. *Methods Enzymol.* **276,** 307–326 (1997).
24. Tong, L. REPLACE, a suite of computer programs for molecular-replacement calculations. *J. Appl. Crystallogr.* **26,** 748–751 (1993).
25. Brunger, A. T. *et al.* Crystallography & NMR system: A new software suite for macromolecular structure determination. *Acta Crystallogr. D* **54,** 905–921 (1998).
26. Jones, T. A., Zou, J.-Y., Cowan, S. W. & Kjeldgaard, M. Improved methods for building models in electron density maps and the location of errors in those models. *Acta Crystallgr. A* **47,** 110–119 (1991).
27. Evans, S. V. SETOR: hardware-lighted three-dimensional solid model representations of macromolecules. *J. Mol. Graph.* **11,** 134–138 (1993).
28. Nicholls, A., Sharp, K. A. & Honig, B. Protein folding and association: insights from the interfacial and thermodynamic properties of hydrocarbons. *Proteins* **11,** 281–296 (1991).
29. Haridas, V., Darnay, B. G., Natarajan, K., Heller, R. & Aggarwal, B. B. Overexpression of the p80 TNF receptor leads to TNF-dependent apoptosis, nuclear factor-κB activation, and c-Jun kinase activation. *J. Immunol.* **160,** 3152–3162 (1998).
30. Shevde, N. K., Bendixen, A. C., Dienger, K. M. & Pike, J. W. Estrogens suppress RANK ligand-induced osteoclast differentiation via a stromal cell independent mechanism involving c-Jun repression. *Proc. Natl Acad. Sci. USA* **97,** 7829–7834 (2000).

**Supplementary Information** accompanies the paper on *Nature*'s website (http://www.nature.com/nature).

### Acknowledgements

We thank the structural biology groups at the Memorial Sloan-Kettering Cancer Center for use of the microcalorimeter; Z. Cao for human TRAF6 cDNA; G. Mosialos and E. Kieff for the human GST–CD40ct construct; L. Tong, R. Khayat, Z. Yang and C. Lima for help with diffraction data collection; G. Cheng for discussions; C. Ogata and MacCHESS staff for beamline access and support; T. Burling for maintaining the home X-ray source; V. Burkitt and A. Villa for technical help; and laboratory members of Imgenex for synthesizing the decoy peptides. This work was supported in part by the NIH (Y.C.), an MSTP grant (J.R.A.), start-up funds from the Department of Bioimmunotherapy (B.G.D.) and a Translational Research Grant from the Leukemia and Lymphoma Society (B.G.D.). H.Y. is a postdoctoral fellow from the Revson Foundation. H.W. is a Pew Scholar of biomedical sciences and a Rita Allen Scholar.

### Competing interests statement

The authors declare that they have no competing financial interests.

Correspondence and requests for materials should be addressed to H.W. (e-mail: haowu@med.cornell.edu). The atomic coordinates have been deposited in the Protein Data Bank under accession numbers 1LB4 (native TRAF6), 1LB5 (TRAF6–TRANCE-R complex) and 1LB6 (TRAF6–CD40 complex).

## erratum

# Regulation of *Arabidopsis* cryptochrome 2 by blue-light-dependent phosphorylation

**Dror Shalitin, Hongyun Yang, Todd C. Mockler, Maskit Maymon, Hongwei Guo, Garry C. Whitelam & Chentao Lin**

*Nature* **417**, 763–767 (2002).

In Fig. 4a the third and fourth lanes should have been labelled $R_{60}$ and $B_{60}$ (not $R_{30}$ and $B_{30}$). □

Supplementary Information

1. Affinity measurements by isothermal titration calorimetry (ITC).

| Proteins | Sequence | $K_D$ (μM) |
|---|---|---|
| hCD40* | 216-KKVAKKPTNKAPHPKQEPQEINFPDDLPGS | 59.9 |
| hCD40 | 230-KQEPQEIDF | 84.0 |
| mTRANCE-R | 337-RKIPTEDEY | 78.0 |
| mTRANCE-R | 370-FQEPLEVGE | 770.0 |
| mTRANCE-R | 444-GNTPGEDHE | 763.0 |
| hIRAK | 539-PPSPQENSYV | 518.1 |
| hIRAK | 582-PNQPVESDE | 79.0 |
| hIRAK | 701-RQGPEESDEF | 54.3 |
| hIRAK-2 | 523-SNTPEETDDV | 66.2 |
| hIRAK-M | 475-PSIPVEDDE | 142.2 |

*The entire intracellular domain of CD40 before the known TRAF2-binding site.

1. Mutations at P-2, P0 and P3 positions of a TRAF6-binding site in full-length TRANCE-R produced no effects on NF-κB activation.

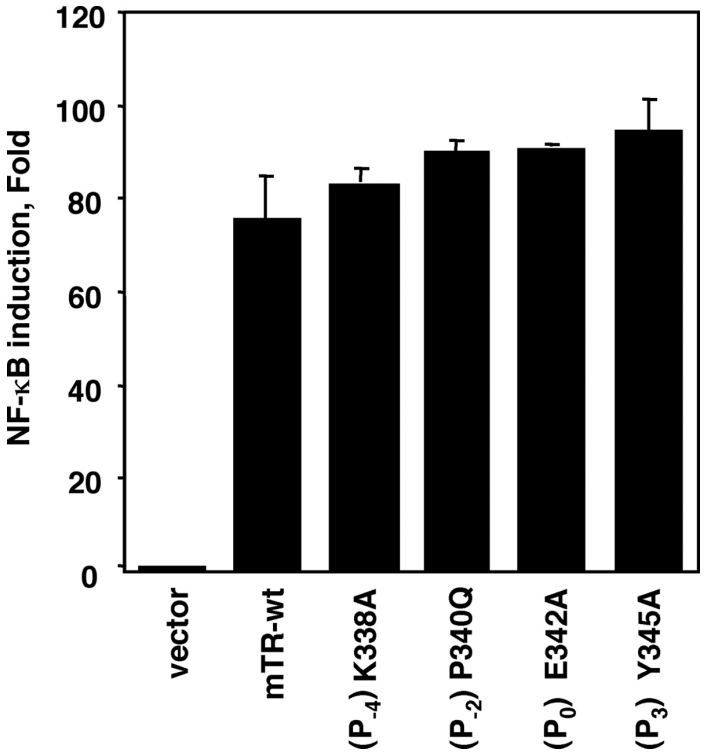

3. Expression levels of wildtype and mutant IRAK and TRAF6 dominant negative (T6.DN), as shown by anti-FLAG immunoblot.

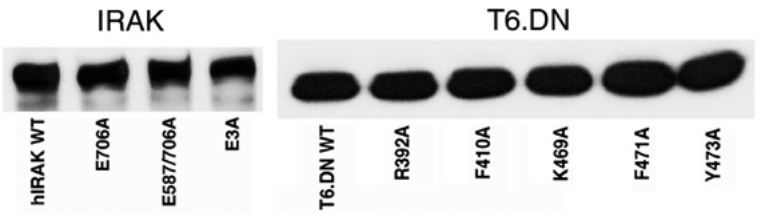


4. Sequence alignment of the TRAF-C domain of TRAF6 and TRAF2. Residues of TRAF6 and TRAF2 involved in receptor interactions are colored. Red: residues with less than 10% side chain surface exposure and more than 20Å$^2$ buried interfacial surface area; magenta: residues with 10-40% side chain surface exposure and more than 20Å$^2$ buried interfacial surface area; green: remaining interface residues. TRAF6 residues that completely abolished CD40 binding when mutated to alanines are labeled by filled circles, while those that did not are shown by open circles.

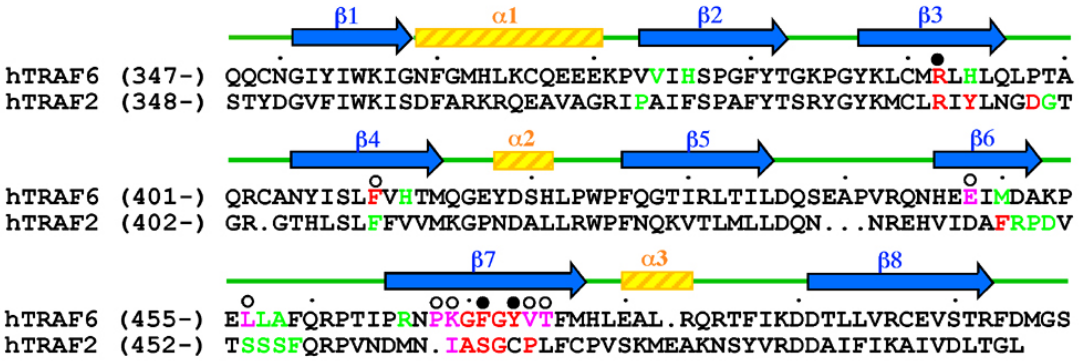

5. Raw264.7 cells were treated with various doses of peptides for 5 days. The cell viability was determined by crystal violet assays (Aggarwal, B. B.. 1985. Human lymphotoxin. Methods Enzymol. 116:441). L-T6DP-1-WT is the peptide used in our study, while T6DP-1 is the same peptide without the leader sequence and therefore does not enter cells and L-T6DP-1-Mut is the triple alanine mutant of L-T6DP-1-WT at positions P-2, P0 and P3 of the TRAF6-binding motif.